MULTIEDGE DETECTION IN SAR IMAGES

Roger Fjørtoft[1,2] *Philippe Marthon*[1] *Armand Lopès*[2] *Eliane Cubero-Castan*[3]

[1]ENSEEIHT (LIMA-IRIT-URA CNRS 1399), 2 rue Camichel, Bp 7122, 31071 Toulouse cedex 7, France
Phone: (33) 5-61-58-83-53 Fax: (33) 5-61-58-83-53 E-mail: Roger.Fjortoft@enseeiht.fr Philippe.Marthon@enseeiht.fr

[2]CESBIO (UMR 5639 CNES/CNRS/UPS), 18 avenue Edouard Belin, Bpi 2801, 31401 Toulouse cedex 4, France
Phone: (33) 5-61-55-85-39 Fax: (33) 5-61-55-85-00 E-mail: Armand.Lopes@cesbio.cnes.fr

[3]CNES – French Space Agency (DGA/SH/QTIS), 18 avenue Edouard Belin, 31401 Toulouse cedex 4, France
Phone: (33) 5-61-27-46-12 Fax: (33) 5-61-27-31-67 E-mail: Eliane.Cubero-Castan@cnes.fr

ABSTRACT

Edge detection is a fundamental issue in image analysis. Due to the presence of speckle, which can be modelled as a strong multiplicative noise, edge detection in Synthetic Aperture Radar (SAR) images is very difficult and methods developed for optical images are inefficient. We here propose a new edge detector for SAR images which is optimum in the MSSE sense for a stochastic multiedge model. It computes a normalized Ratio Of Exponentially Weighted Averages (ROEWA) on opposite sides of the central pixel. This is done in the horizontal and vertical direction, and the module of the two components yields an edge strength map. Thresholding of the edge strenght map and postprocessing to eliminate false edges are briefly discussed. We present results on simulated SAR images and ERS1 data.

1. INTRODUCTION

We shall start from a general image processing viewpoint and incorporate the specific properties of SAR images as we go along. In optical images without texture, an edge pixel is usually defined as a local maximum of the gradient module in the direction of the gradient, or equivalently, as a zero-crossing of the second derivative in the gradient direction. Prior to the derivation, smoothing is necessary, as differential operators are sensitive to noise.

For simplicity, we restrict ourselves to separable filters. Let f be a one-dimensional smoothing filter and g its first derivative. The horizontal and the vertical component of the gradient of the smoothed image are given by:

$$\Delta_x[(f(x)f(y)) \otimes I(x,y)] = g(x) * (f(y) \star I(x,y)) \quad (1)$$

$$\Delta_y[(f(x)f(y)) \otimes I(x,y)] = g(y) \star (f(x) * I(x,y)) \quad (2)$$

Here, $\otimes$ denotes bidimensional convolution, $*$ denotes convolution in the horizontal direction and $\star$ denotes convolution in the vertical direction. Basically, each component of the gradient corresponds to the difference of the local mean values computed on opposite sides of the central pixel.

The signal to noise ratio is very low in SAR images, typically 0 dB for one-look images. To sufficiently reduce the influence of the speckle, the smoothing window must contain an important number of pixels. Unfortunately, large windows tend to blur the edges and subsequently reduce the edge localisation precision. The filter should be designed to optimize the compromise between noise suppression and spatial resolution. The multiplicative nature of speckle must be taken into account explicitely.

2. MULTIEDGE MODEL

As the sliding window on which the smoothing is performed is large, it is likely to contain several edges. The frequently used mono-stepedge model is therefore inappropriate. A statistical multiedge model is more realistic. We suppose that the reflectivity (ideal image) R is a stationary random process composed by piecewise constant segments with random magnitudes $\{r_i\}$, with mean value μ_r and standard deviation σ_r. The localization of the reflectivity jumps $\{x_i\}$ follows a Poisson distribution with parameter λ corresponding to the mean jump frequency. The local reflectivities $\{r_i\}$ and the jump localizations $\{x_i\}$ are supposed to be independent. Hence $\mu_R = \mu_r$ and $\sigma_R = \sigma_r$.

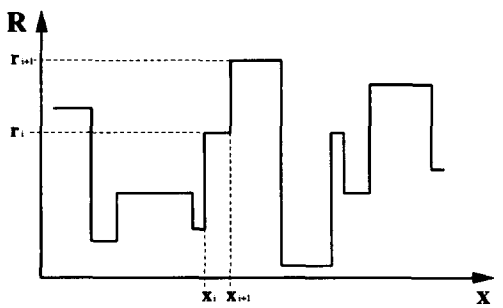

Figure 1. The one-dimensional multiedge model.

It can easily be shown that the autocovariance function of the reflectivity is:

$$C_{RR}(\Delta x) = \sigma_R^2 e^{-\lambda|\Delta x|} \quad (3)$$

The power spectral density, which we here define as the Fourier transform of the autocovariance function, is then:

$$S_{RR}(\omega) = \frac{2\lambda\sigma_R^2}{\lambda^2 + \omega^2} \quad (4)$$

3. MULTIPLICATIVE NOISE MODEL

Speckle is due to the constructive and destructive interference between the responses of the different elementary scatterers in a resolution cell. It is well modelled as a multiplicative random noise n in intensity images [1]:

$$I(x) = R(x) \cdot n(x) \quad (5)$$

Copyright 1997 IEEE

The transfer function of the SAR system is designed to vary as little as possible over the bandwidth of interest. It changes the spectrum of the ideal image very little, but limits the bandwidth of the noise spectrum. This effect is here incorporated in the term n. Speckle is gamma distributed with $\mu_n = 1$ and $\sigma_n^2 = 1/L$, where L is the equivalent number of looks [1]. The autocorrelation of the speckle decreases very rapidly. As an approximation, n will be considered as white noise in what follows:

$$C_{nn}(\Delta x) = \sigma_n^2 \delta(\Delta x) \tag{6}$$

$$S_{nn}(\omega) = \sigma_n^2 \tag{7}$$

4. LINEAR MMSE FILTER

The best unbiased linear estimator of the reflectivity has the form [2, 3]:

$$\hat{R}(x) = \mu_R(x) + f(x) * (I(x) - \mu_I) \tag{8}$$

Minimizing the mean square error yields the optimum transfer function [3]:

$$F(\omega) = \frac{\mu_n S_{RR}(\omega)}{S_{RR}(\omega) * S_{nn}(\omega) + \mu_R^2 S_{nn}(\omega) + \mu_n^2 S_{RR}(\omega)} \tag{9}$$

By substituting into eq. (9) and taking the inverse Fourier transform we obtain the optimum impulse response:

$$f(x) = Ce^{-\alpha|x|}, \tag{10}$$

where

$$\alpha^2 = \frac{2L\lambda}{1 + (\mu_R/\sigma_R)^2} + \lambda^2 \tag{11}$$

and C is a constant. The unknown parameters can be estimated from the measured intensity image or a speckle reduced image obtained by adaptive filtering [4].

We normalize f with respect to the mean value, *ie* $C = \alpha/2$, to obtain a non-biased estimate. With this normalization eq. (8) simplifies to

$$\hat{R}(x) = f(x) * I(x). \tag{12}$$

The filter f is known as the Infinite Symmetric Exponential Filter (ISEF) [5]. Its first derivative is given by:

$$g(x) = \frac{d}{dx} f(x) = \begin{cases} K \cdot e^{-\alpha x} & \text{if } x > 0 \\ -K \cdot e^{\alpha x} & \text{if } x < 0 \end{cases} \tag{13}$$

where K is a constant. The filters f and g, together with eq. (1) and (2), define the edge detector of Shen and Castan [5], which is an optimum multiedge detector for images degraded by additive white noise. It is claimed to give better edge localization precision than other edge detectors proposed for images with additive noise. The filter $f(x)$ and its first derivative $g(x)$ are shown in fig. 2. In the discrete case, they can both be implemented very efficiently by a pair of first order Infinite Impulse Response (IIR) filters, $f_1(n)$ and $f_2(n)$, realizing the normalized causal and anti-causal part of $f(n)$, respectively [4, 5, 6].

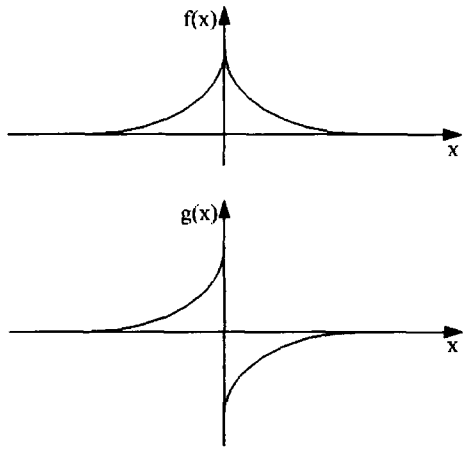

Figure 2. The ISEF filter and its first derivative

5. EDGE DETECTION

Owing to the multiplicative nature of speckle, edge detectors based on the *difference* of local mean values detect more false edges in areas of high reflectivity than in areas of low reflectivity. Several *monoedge* detectors with Constant False Alarm Rate (CFAR) have been developed for SAR images, *eg* based on a normalized Ratio Of Averages (ROA) [7] or a Likelihood Ratio (LR) [8]. Oliver *et al* recently showed that the LR detector for gamma distributed speckle coincides with the ROA operator when only the averages are calculated on equal sized halves of the analyzing window [8].

To obtain a spatially optimum *multiedge* detector with CFAR, we can take the normalized *ratio* rather than the difference of the outputs of the filters f_1 and f_2 in the differentiation step, *cf* eq. (1) and (2) and fig. 2. To compute the horizontal edge strength component, the image is first smoothed column by column using the one-dimensional smoothing filter f, Next, the filters f_1 and f_2 are employed independently line by line on the result of the smoothing operation, and the ratio of their outputs is calculated for each pixel. The ratio is normalized to be superior to one by taking the maximum of the computed ratio and its inverse. The vertical edge strength component is obtained in the same manner, except that the directions are interchanged. The module of the components gives the edge strength map.

The segmentation is obtained from the edge strength map by a modified version of the *watershed algorithm* [9], which is a simple and efficient edge detection method which yields closed, skeleton boundaries running through local maxima of the edge strength map. The modification consists in introducing a detection threshold [4, 10]. Only edge strengths over the chosen threshold are considered. Local maxima with lower magnitudes are supposed to be due to noise. For the modified watershed algorithm to form meaningful boundaries, the edge detection threshold must be set relatively low. Consequently, numerous false edges will also be detected.

6. POSTPROCESSING

False edges can be eliminated by merging regions whose mean values are not significantly different. The LR for re-

Copyright 1997 IEEE

gion merging is simply the inverse of the LR for edge detection [4, 8]. Geometrical considerations can also be taken into account, based on *a priori* knowledge about the size and shape of the regions. The order in which the regions are merged is very important. A computionally efficient and locally optimum approach is the iterative pairwise mutually best merge criterion [11].

7. EXPERIMENTAL RESULTS

The novelty of the ROEWA operator compared to other CFAR detectors is that it relies on exponentially weighted means rather than arithmetic means. To study the influence of this weighting we compare it with the ROA detector.

Let us first consider a "cartoon image" composed of vertical lines of linearly increasing width shown in fig. 3. The ratio between the reflectivities of the bright and the dark lines is 4. Its 1-look speckled counterpart was simulated with approximate ERS1 caracteristics. With $e^{-\alpha} = 0.9$ for the ROEWA operator and window size 37×37 for the ROA operator we have the same equivalent number of independent pixels [4] in each half window, and thus the same speckle supression capacity for both operators. The edges were detected by the modified watershed algorithm with threshold 1.6. As all real edges are vertical, the number of horizontal edges gives a visual appreciation of the false alarm rate. We see that it is approximately the same for both operators. The ROEWA operator gives a systematic detection of edges for a line width of 7 or higher, whereas the the ROA operator detects systematically only from line width 12. The experiment indicates that the ROEWA operator has better spatial resolution than the ROA operator for a given speckle reduction capacity.

The operators were also tested on a multitemporal series of 3-look ERS1 images of an agricultural scene near Bourges, France. Visual inspection revealed small differences, the ROEWA operator giving only slightly better results than the ROA operator. The best results were obtained with $e^{-\alpha} = 0.73$ and window size 13×13, respectively, for which the two operators had the same speckle reduction capacity. We allowed a massive over-segmentation in the edge detection step, and then eliminated false edges by merging regions according to the LR criterion. Regions containing only one pixel were supposed to be due to speckle and merged without further testing. The result for the ROEWA operator is shown in fig. 4.

8. CONCLUSION

In this paper, we propose an optimum multiedge detector for radar images, the ROEWA operator. It was tested on simulated SAR images, where it detected edges on finer scales than the ROA operator. Rather than estimating arithmetic averages on finite size windows, as other CFAR detectors do, the ROEWA operator computes exponentially weighted local mean values over infinite size windows. Thanks to the exponentially decaying weighting function, this can be done without the loss of localization precision which usually limits the use of large windows. Combined with watershed thresholding and region growing, the ROEWA operator yields thematic segmentations which can be exploited in speckle reduction [12] and classification [13].

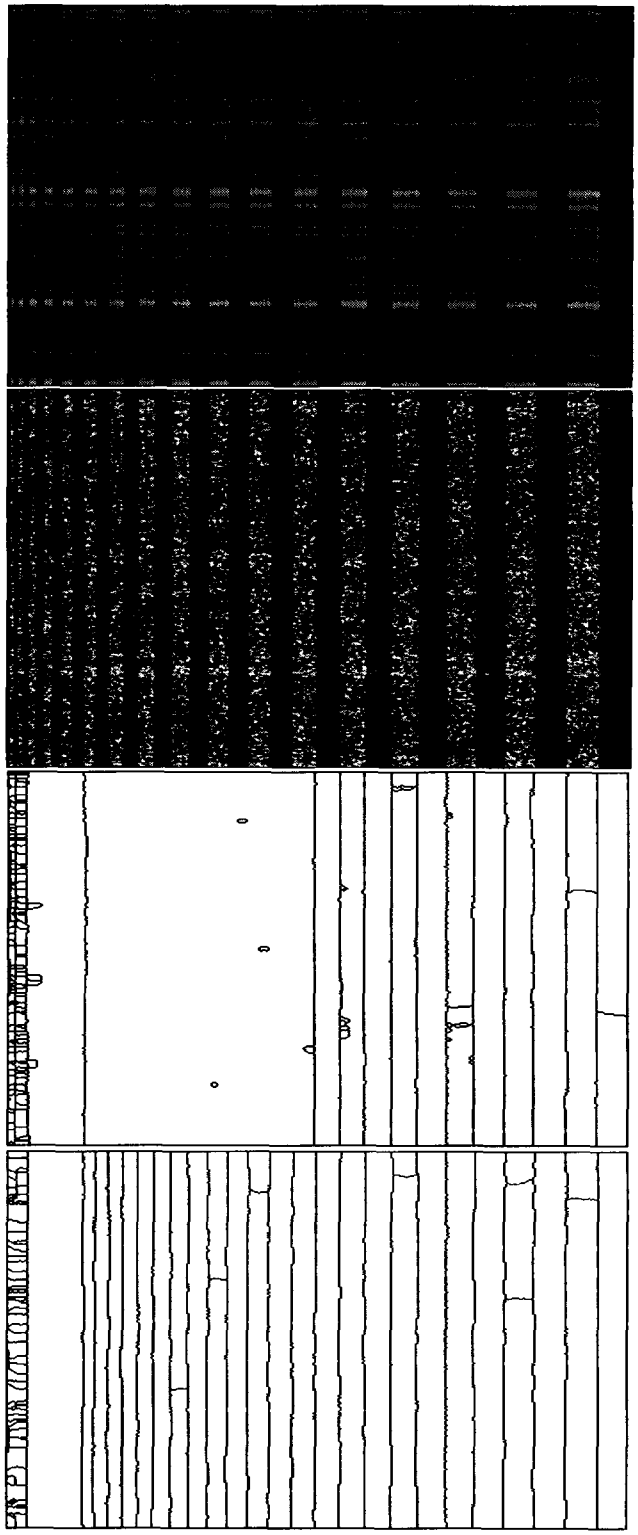

Figure 3. Ideal image consisting of vertical lines of width 2 to 18 (top), simulated 1-look SAR image, segmentation obtained with the ROA edge detector, and segmentation obtained with the ROEWA edge detector (bottom).

Copyright 1997 IEEE

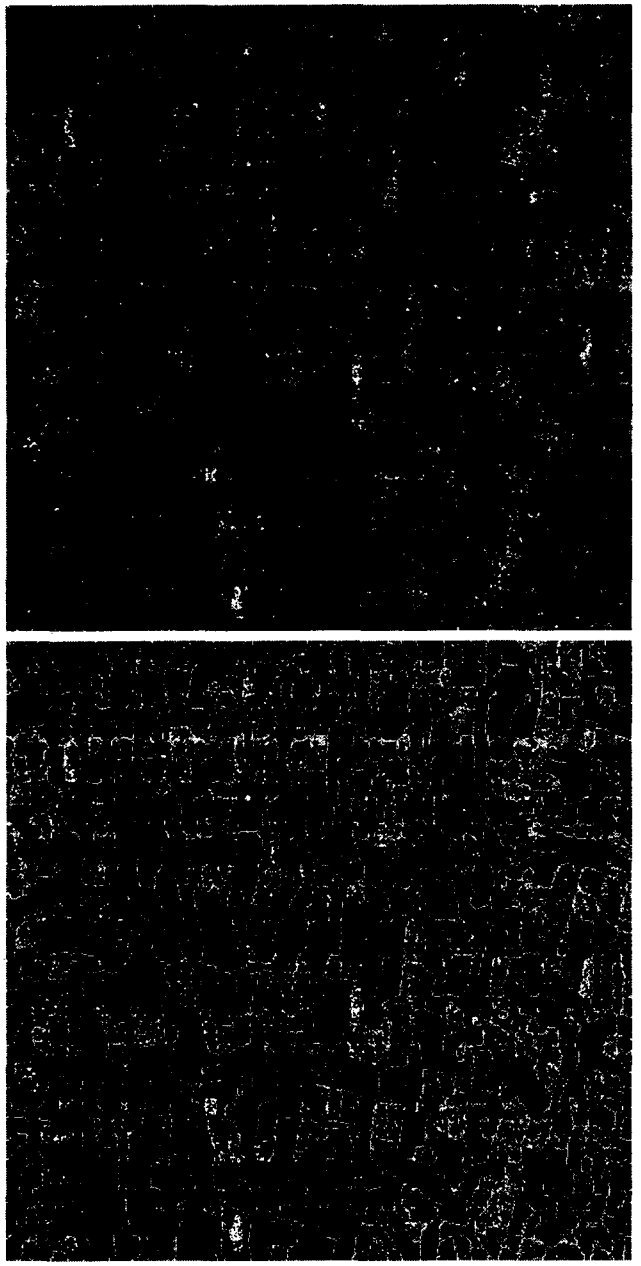

Figure 4. SAR image of an agricultural scene near Bourges, France, ©ESA - ERS1 data - 1993 - Distribution SPOT IMAGE, and segmentation obtained by the ROEWA operator, watershed thresholding and LR region merging. The CD-ROM version shows a colour composition of three dates.

ACKNOWLEDGMENTS

This study was realized by CESBIO and LIMA/ENSEEIHT under contract 833/CNES/94/1022/00. The authors thank Danielle Ducrot-Gambart, Franck Sery, Nathalie Mauduit and José Christophe Cabada for the co-operation.

REFERENCES

[1] F. T. Ulaby, R. K. Moore, and A. K. Fung, *Microvave Remote Sensing*, vol 3, Dedham, MA: Artech House, 1986.

[2] V. S. Frost, K. S. Shanmugan, and J. C. Holtzman, "A model for radar images and its application to adaptive filtering of multiplicative noise," *IEEE Trans. PAMI*, vol. 4, no. 2, pp. 165-177, March 1982.

[3] J. W. Woods and J. Biemond, "Comments on "A model for radar images and its application to adaptive filtering of multiplicative noise"," *IEEE Trans. PAMI*, vol. 6, no. 5, pp. 658-659, September 1984.

[4] R. Fjørtoft, A. Lopès, P. Marthon and E. Cubero-Castan, "Optimum Multiedge Detection for SAR Image Segmentation," submitted to *IEEE Trans. Geosci. Remote Sensing*, 1996.

[5] J. Shen and S. Castan, "An optimal linear operator for step edge detection," *CVGIP: Graphical Models Image Process.*, vol. 54, no. 2, pp. 112-133, March 1992.

[6] R. Fjørtoft, P. Marthon, A. Lopès, and E. Cubero-Castan, "Edge detection in radar images using recursive filters," in *Proc. ACCV*, vol. 3, Singapore, December 1995, pp. 87-91.

[7] R. Touzi, A. Lopès, and P. Bousquet, "A statistical and geometrical edge detector for SAR images," *IEEE Trans. Geosci. Remote Sensing*, vol. 26, no. 6, pp. 764-773, november 1988.

[8] C. J. Oliver, D. Blacknell, and R. G. White, "Optimum edge detection in SAR," *IEE Proc. Radar Sonar Navig.*, vol. 143, no. 1, February, 1996.

[9] L. Vincent and P. Soille, "Watersheds in digital spaces: An efficient algorithm based on immersion simulations," *IEEE Trans. PAMI*, vol. 13, no. 6, pp. 583-598, 1991.

[10] P. Marthon, B. Paci, and E. Cubero-Castan, "Finding the structure of a satellite image," in *Proc. EurOpto Image and Signal Processing for Remote Sensing*, vol. SPIE 2315, Rome, Italy, 1994, pp. 669-679.

[11] A. Baraldi and F. Parmiggiani, "Segmentation driven by an iterative pairwise mutually best merge criterion," in *Proc. IGARSS*, Firenze, Italy, July 1995, pp. 89-92.

[12] R. Fjørtoft, F. Lebon, Franck Sery, A. Lopès, P. Marthon, and E. Cubero-Castan, "A region-based approach to the estimation of local statistics in adaptive speckle filters," in *Proc. IGARSS*, Lincoln, Nebraska, May 1996, pp. 457-459.

[13] Franck Sery, A. Lopès, D. Ducrot-Gambart, R. Fjørtoft, E. Cubero-Castan, and P. Marthon, "Multisource classification of SAR images with the use of segmentation, polarimetry, texture and multitemporal data," in *Proc. EurOpto Image and Signal Processing for Remote Sensing*, vol. SPIE 2955, Taormina, Italy, September, 1996.

Copyright 1997 IEEE